

1 **Comparison of the multifractal characteristics of heavy**
2 **metals in soils within two areas of contrasting economic**
3 **activities in China**

4 Xiaohui Li^{a, b}, Xiangling Li^a, Feng Yuan^{a, b*}, Simon M. Jowitt^{c, d}, Taofa Zhou^a, Kui
5 Yang^a, Jie Zhou^a, Xunyu Hu^a, Yang Li^a

6 a. School of Resources and Environmental Engineering, Hefei University of
7 Technology, Hefei 230009, China

8 b. Xinjiang Research Centre for Mineral Resources, Xinjiang Institute of Ecology and
9 Geography, Chinese Academy of Sciences, Urumqi, Xinjiang 830011, China

10 c. School of Earth, Atmosphere and Environment, Monash University, Wellington
11 Road, Clayton, VIC 3800, Australia

12 d. Department of Geoscience, University of Nevada Las Vegas, 4505 S. Maryland
13 Parkway, Las Vegas, NV 89154-4010, USA

14 *Corresponding author: Email: yf_hfut@163.com, Tel: +8605512901648

15 **Abstract**

16 Industrial and agricultural activities can generate heavy metal pollution that can
17 cause a number of negative environmental and health impacts. This means that
18 evaluating heavy metal pollution and identifying the sources of these pollutants,
19 especially in urban or developed areas, is an important first step in mitigating the
20 effects of these contaminating but necessary economic activities. Here, we present the
21 results of a heavy metal (Cu, Pb, Zn, Cd, As and Hg) soil geochemical survey in Hefei
22 city. We used a multifractal spectral technique to identify and compare the
23 multifractality of heavy metal concentrations of soils within the industrial Daxing and
24 agricultural Yicheng areas. This paper uses three multifractal parameters ($\Delta\alpha$, $\Delta f(\alpha)$
25 and $\tau''(1)$) to indicate the overall amount of multifractality within the soil geochemical

26 data. The results show all of the elements barring Hg have larger $\Delta\alpha$, $\Delta f(\alpha)$ and $\tau''(1)$
27 values in the Daxing area compared to the Yicheng area. The degree of multifractality
28 suggests that the differing economic activities in Daxing and Yicheng generate very
29 different heavy metal pollution loads. In addition, the industrial Daxing area contains
30 significant Pb and Cd soil contamination, whereas Hg is the main heavy metal present
31 in soils within the Yicheng area, indicating that differing clean-up procedures and
32 approaches to remediating these polluted areas are needed. The results also indicate
33 that multifractal modeling and the associated generation of multifractal parameters
34 can be a useful approach in the evaluation of heavy metal pollution in soils.

35

36 **Keywords:** soil geochemistry; multifractal modelling; heavy metal pollution; Hefei

37

38 **1. Introduction and overview of the study area**

39 Heavy metal pollution within soil poses a serious risk for human health and the
40 environment, and thus soil pollution caused by anthropogenic activities (including
41 industry and agriculture) has been the focus of a significant amount of research (e.g.,
42 [Leyval et al., 1997](#); [Thomas and Stefan, 2002](#); [McGrath et al., 2004](#); [Wang et al., 2007](#);
43 [Luo et al., 2011](#)). Analyzing soil geochemistry and pollution using multifractal
44 techniques may allow for assessing many of the problems of nonlinear variability
45 which commonly arise when dealing with pollutants, as well as enabling the
46 identification of non-linear characteristics within datasets. This approach can yield
47 new information that can be used to understand the factors controlling the distribution
48 of key elements within the objects or data being studied ([Salvadori, 1997](#); [Gonçalves,](#)
49 [2000](#); [Zuo et al., 2012](#)). This in turn means that determining the multifractal
50 characteristics of the distribution of heavy metals in soils can improve our
51 understanding of any heavy metal pollution that is associated with these differing
52 anthropogenic activities.

53 Multifractal techniques include singularity mapping and multifractal
54 interpolation that enable more detailed analysis of the spatial distribution of heavy

55 metals, concentration-area modeling that can be used to define threshold values
56 between background (i.e. geological) and anthropogenic anomalies (Lima et al., 2003),
57 spectral density-area modeling that can be used to define thresholds to separate
58 anomalies (i.e., anthropogenically derived heavy metal concentrations in this case)
59 from background concentrations (i.e., geologically derived heavy metal
60 concentrations; Cheng, 2001), and multifractal spectra that highlights non-linear
61 characteristics and identifies anomalous behavior that reflects the characteristics of
62 some multifractal sets (Gonçalves, 2000; Albanese et al., 2007; Guillén et al., 2011),
63 such as the presence of porous structures and spatial variations in soil properties
64 (Caniego et al., 2005; Dathe et al., 2006). This means that multifractal techniques can
65 be useful tools for the analysis of heavy metal pollution within soils (e.g., Salvadori et
66 al., 1997; Lima et al., 2003; Albanese et al., 2007; Guillén et al., 2011). These
67 multifractal techniques are not only used in environmental science, but also in a
68 number of differing fields, including geophysics (Schertzer et al., 2011), medicine
69 (Jennane et al., 2001), computer science (Wendt et al., 2009), geology (Cheng, 1995;
70 Deng et al., 2011; Yuan et al., 2012, 2015) and ecology (Pascual et al., 1995), among
71 others.

72 Hefei is the capital of Anhui Province, China, and has an urban area that includes
73 the towns of Daxing and Yicheng, which focus on industrial and agricultural activities,
74 respectively. Here, we use multifractal spectra techniques and three parameters ($\Delta\alpha$,
75 $\Delta f(\alpha)$ and $\tau''(1)$) to analyze and compare the degree and characteristics of the
76 multifractality of heavy metal contamination in soils associated with anthropogenic
77 activities in this region. The results will further enable and inform future planning for
78 any necessary remediation of the soils in the Daxing and Yicheng areas.

79

80 **2. Study area and geochemical data**

81 **2.1 Study area**

82 The city of Hefei is situated in central–eastern China (Fig. 1(a)), has
83 approximately 7.7 million inhabitants and covers an area of around 11,408 km². This

84 paper focuses on the towns of Daxing and Yicheng (Fig. 1(b)), with the former
85 representing one of the traditional industrial areas of Hefei and containing numerous
86 factories that are involved in the steel industry, chemical industry, paper making, and
87 the production of furniture and construction materials, among others. In contrast, the
88 town of Yicheng focuses its economic activities on agricultural production, byproduct
89 processing, livestock and poultry breeding, ornamentals, and other enterprises related
90 to agricultural activity.

91 **2.2 Sampling and analysis**

92 The study areas are covered by Quaternary sedimentary soils and are free of both
93 natural mineralization and mining-related contamination. A total of 169 surface (<20
94 cm depth) soil samples were taken from the towns of Daxing and Yicheng on 1 × 1
95 km grids, yielding 78 samples from Daxing and 91 samples from Yicheng (Fig.
96 1(c–d)). Sampling errors were minimized by splitting each sample into 3–5
97 sub-samples, each of which weighed more than 500 g. Each of these sub-samples was
98 air-dried before being broken up using a wooden roller and then sieved to pass
99 through a 0.85 mm mesh. The concentrations of 6 heavy metal elements (Cu, Pb, Zn,
100 Cd, As and Hg) were determined during this study, with Cd, Cu, Pb and Zn
101 concentrations determined by inductively coupled plasma–mass spectrometry
102 (ICP–MS), whereas Hg and As concentrations were determined by hydride
103 generation–atomic fluorescence spectrometry (AFS; Armstrong et al., 1999;
104 Gómez-Ariza et al., 2000). These techniques have detection limits of 1 ppm for Cu, 2
105 ppm for Pb and Zn, 30 ppb for Cd, 0.5 ppm for As and 5 ppb for Hg. The accuracy of
106 these data was monitored by repeat and replicate determinations using instrumental
107 neutron activation analysis (INAA), with analytical precision monitored using
108 variance of the results obtained from duplicate analyses.

109

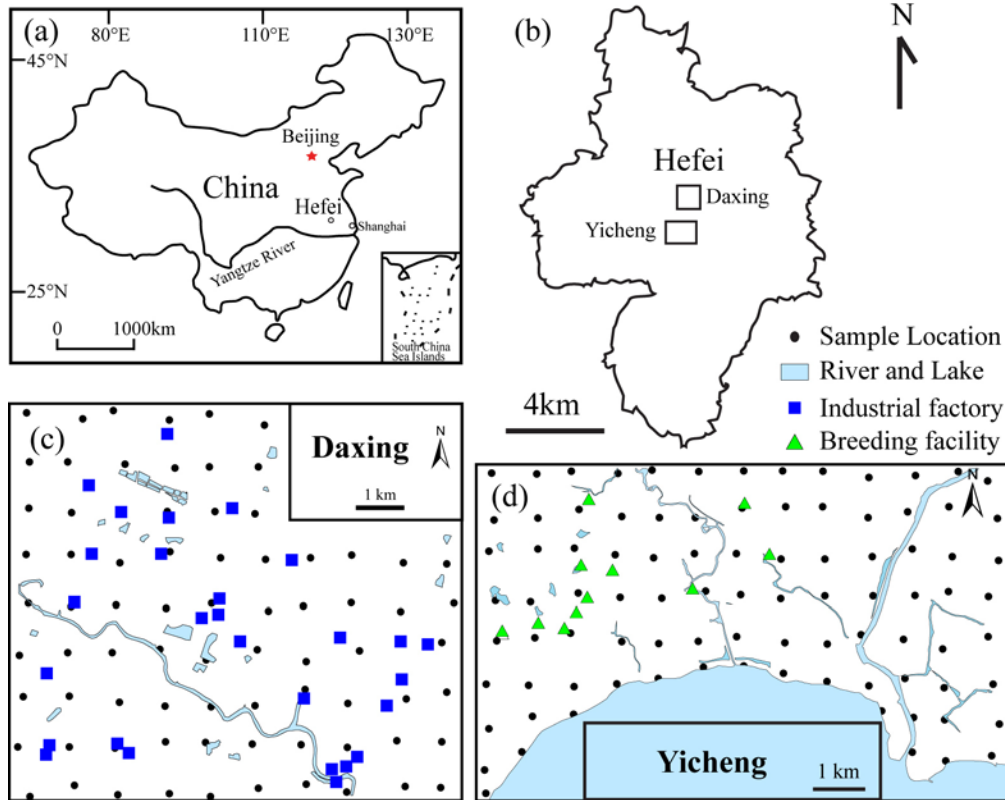


Fig. 1. Location of Hefei in central-eastern China (a); location of the study areas within Hefei (b); the 1 × 1 km grids used for soil sampling in the towns of Daxing (c) and Yicheng (d)

3. Multifractal spectrum analysis

Multifractal formalisms can decompose self-similar measures into intertwined fractal sets that are characterized by singularity strength and fractal dimensions (Cheng, 1999). Using multifractal techniques allows non-linear characteristics within datasets to be identified, enabling the extraction of information that can be used to understand the factors controlling the distribution of key elements within the data. Fractal spectra ($f(\alpha)$) are formalisms that can be used to describe the multifractal characteristics of a dataset and can be estimated using box-counting based moment, gliding box, histogram and wavelet methods, among others (Cheng, 1999; Lopes and Betrouni, 2009). The most widely used of these methods are the box-counting and gliding box methods, both of which are based on the moment method.

The calculation of the mass exponent function $\tau(q)$ for the gliding box method is different from the box-counting method, with the gliding box method providing a

128 useful approach that can increase the number of samples that are available for
 129 statistical estimation within a dataset (Buczowski et al., 1998; Tarquis et al., 2006;
 130 Xie et al., 2010). This means that the gliding box approach often provides better
 131 results with lower uncertainties than the box-counting method (Cheng, 1999). As such,
 132 we have used the gliding box approach during this study. The calculation of the mass
 133 exponent function $\tau(q)$ for the gliding box method uses a partition function as follows
 134 (Cheng, 1999):

$$135 \quad \langle \tau(q) \rangle + D = \lim_{\varepsilon \rightarrow 0} \left(\frac{\log(\mu^q(\varepsilon))}{\log(\varepsilon)} \right) = \lim_{\varepsilon \rightarrow 0} \left(\frac{\log \left(\frac{1}{N^*(\varepsilon)} \sum_{i=1}^{N^*(\varepsilon)} \mu_i^q(\varepsilon) \right)}{\log(\varepsilon)} \right) \quad (1)$$

136 where $\mu_i(\varepsilon)$ denotes a measure with the i_{th} cell of a gliding box of size ε , q is the order
 137 moment of this measure (this paper used a range of q values from -10 to 10 with an
 138 interval of 1), $\langle \rangle$ indicates the statistical moment, and $N^*(\varepsilon)$ indicates the total
 139 number of gliding boxes of size ε with $\mu_i(\varepsilon)$ values different from 0 .

140 The values of $\tau(q)$ derived using this equation can be then used to determine
 141 singularity α and fractal spectra $f(\alpha)$ values using a Legendre transformation, as
 142 expressed below:

$$143 \quad \alpha(q) = \frac{d\tau(q)}{dq} \quad (2)$$

$$144 \quad f(\alpha) = q\alpha(q) - \tau(q) = q \frac{d\tau(q)}{dq} - \tau(q) \quad (3)$$

145 $\Delta\alpha$ and Δf are essential parameters required to analyze the multifractal
 146 characteristics of a given dataset. The widths of the left ($\Delta\alpha_L$) and right ($\Delta\alpha_R$) branches
 147 within the multifractal spectra are then defined using the following equations:

$$148 \quad \Delta\alpha_L = \alpha_0 - \alpha_{\min} \quad (4)$$

$$149 \quad \Delta\alpha_R = \alpha_{\max} - \alpha_0 \quad (5)$$

$$150 \quad \Delta\alpha = \alpha_{\max} - \alpha_{\min} \quad (6)$$

151 and the height difference $\Delta f(\alpha)$ between the two ends of the multifractal spectrum is

152 then extracted using:

$$153 \quad \Delta f(\alpha) = f(\alpha_{\max}) - f(\alpha_{\min}) \quad (7)$$

154 Higher $\Delta\alpha$ and $\Delta f(\alpha)$ values are generally indicative of datasets with more
155 heterogeneous patterns (ordered, complex, clustered) and higher levels of
156 multifractality (Cheng, 1999; Kravchenko et al., 1999). In addition, local
157 multifractality $\tau''(1)$, which may determined by ordinary spatial analysis functions
158 (autocorrelations and semivariograms), can also be used as a measure to quantitatively
159 characterize the multifractality of a dataset using equation 8 (Cheng, 2006):

$$160 \quad \tau''(1) = \tau(2) - 2\tau(1) + \tau(0) \quad (8)$$

161 If μ is a multifractal and $-D < \tau''(1) < 0$, where D is the gliding-box dimension,
162 then more negative values of $\tau''(1)$ are indicative of higher degrees of multifractality,
163 whereas otherwise $\tau''(1) = 0$ for monofractal.

164

165 **4. Geochemical analysis results**

166 A statistical summary of the soil geochemical data for the study area is given in
167 [Table 1](#). Samples from the Daxing area have higher Cu, Pb, Zn, Cd and As maximum,
168 mean, standard deviation, skewness, and kurtosis values than soil samples from the
169 Yicheng area, whereas the Yicheng area has a higher maximum Hg concentration
170 value than the Daxing area. In addition, the soil samples from Daxing have much
171 higher coefficient of variation (CV) values for Cu, Pb, Zn, Cd and As than the
172 samples from the Yicheng area, indicating that soils in the Daxing area contain higher
173 and more variable concentrations of these elements. This also suggests that samples
174 from the Daxing area containing elevated concentrations of heavy metals were
175 probably contaminated by anthropogenic activity.

176 All of the elements (barring Pb and Cu in the Yicheng area) in both the Yicheng
177 and Daxing areas yielded concentration histograms that are positively skewed and
178 contain some outliers (Fig. 2), indicating that these data have non-normal and
179 potentially fractal- or multifractal-type distributions. This means that multifractal

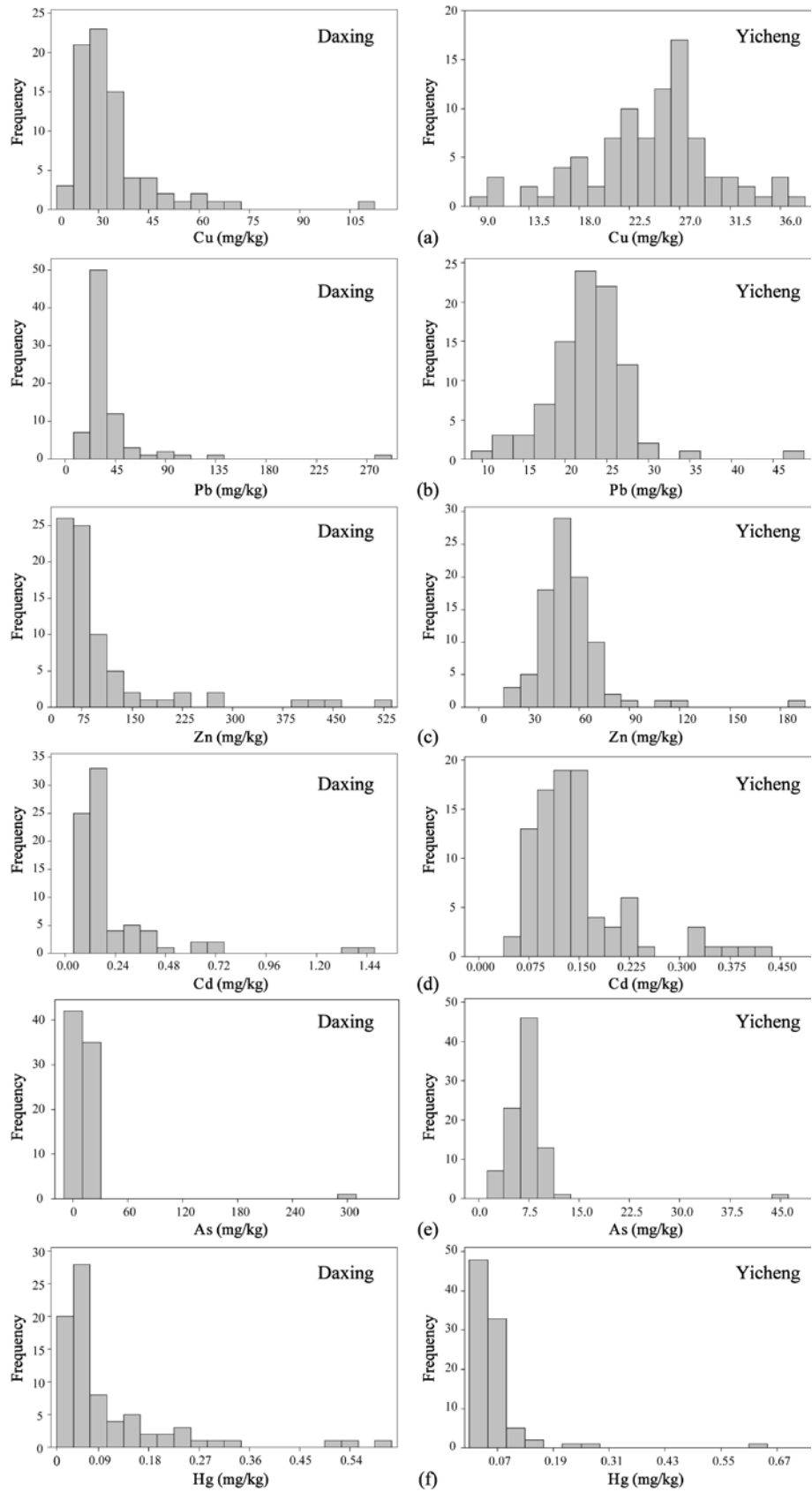
180 techniques are highly suited for the characterization of the geochemistry of the soils.

181

182 **Table 1.** Summary statistics of soil heavy metal concentrations within samples from the Daxing
183 and Yicheng areas.

Town	Element	Min	Max	Mean	Standard deviation	Skewness	Kurtosis	CV*
		(mg/kg)	(mg/kg)	(mg/kg)	-	-	-	(%)
Daxing	Cu	19.00	111.50	33.87	13.26	3.20	14.93	39.16
	Pb	18.90	291.30	39.57	35.03	5.37	35.41	88.51
	Zn	40.90	526.10	105.8	94.40	2.91	8.59	89.19
	Cd	0.045	1.48	0.23	0.24	3.45	13.81	108.23
	As	4.93	308.20	13.97	33.89	8.72	76.64	242.56
	Hg	0.03	0.60	0.11	0.11	2.68	7.78	107.29
Yicheng	Cu	9.60	37.80	24.34	5.77	-0.38	0.41	23.71
	Pb	10.40	46.30	22.77	4.91	0.87	5.51	21.56
	Zn	20.80	194.80	54.70	21.43	3.45	20.27	39.17
	Cd	0.054	0.43	0.15	0.08	1.84	3.49	51.85
	As	2.30	44.20	7.29	4.39	6.68	56.55	60.24
	Hg	0.02	0.62	0.06	0.07	5.75	41.26	113.09

184 *CV: coefficient of variation.



185

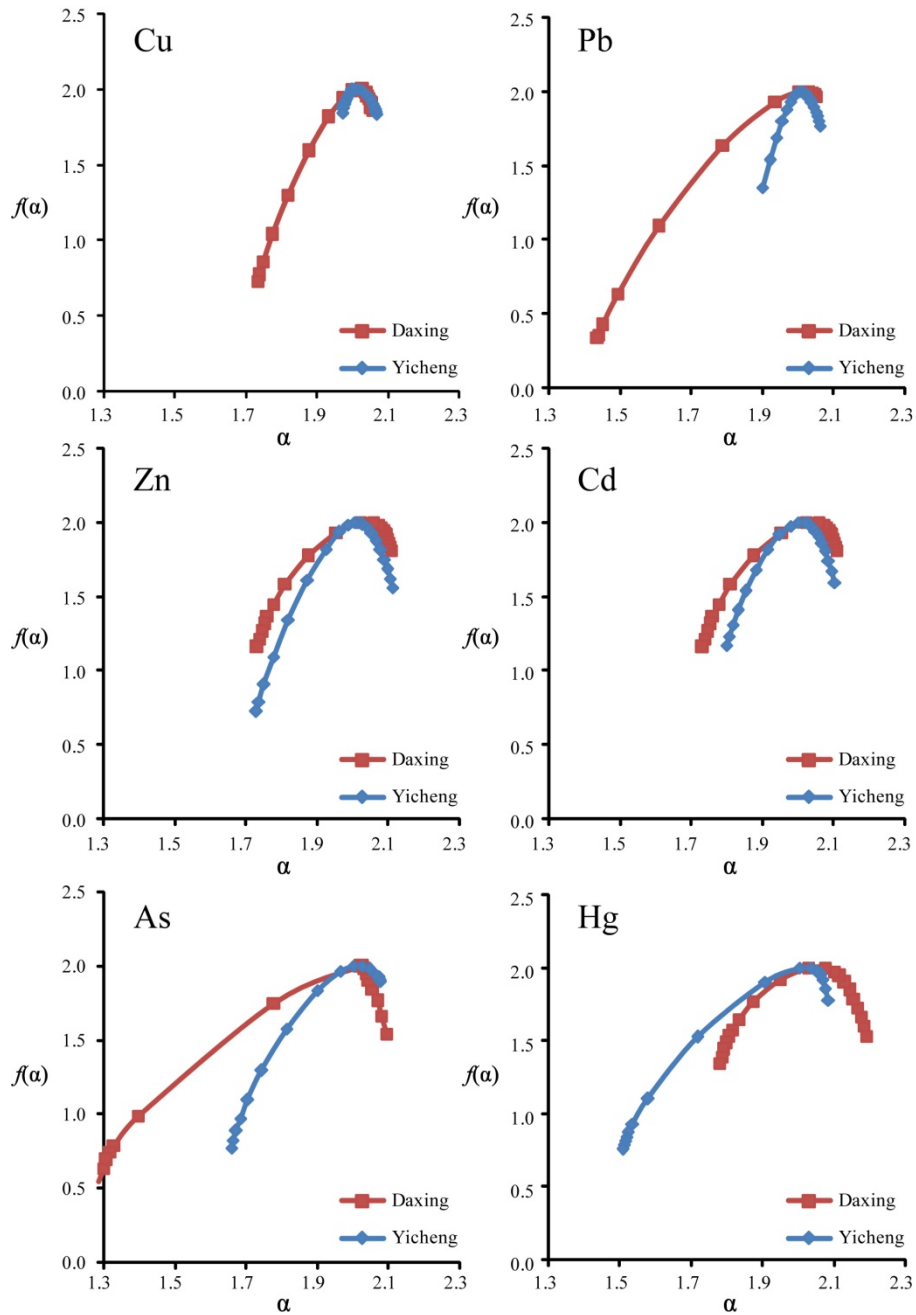
186 **Fig. 2.** Histograms showing the distribution of Cu (a), Pb (b), Zn (c), Cd (d), As (e) and Hg (f)
 187 concentrations within soils from the towns of Daxing and Yicheng.

188

189 **5. Calculation processes of multifractal spectrum and discussion**

190 The multifractal spectra (in the form of an α - $f(\alpha)$ diagram) for the geochemical
 191 data are shown in Fig. 3.

192



193

194 **Fig. 3.** Multifractal spectra ($f(\alpha)$ vs α) of the soil geochemical data from the Daxing and Yichen
 195 area.

196

197 These multifractal spectra have inverse bell shapes (Fig. 3) and are asymmetric
 198 (i.e. $\Delta\alpha_L$ values significantly differ from $\Delta\alpha_R$, equations 5-6) with the exception of the

199 Cu data for soils from the Yicheng area, indicating that the samples containing low
200 and high concentrations of these elements are not evenly distributed within the study
201 area (as is expected for areas containing point source pollutants like factories or
202 animal breeding facilities).

203 The multifractal results given in Table 2 indicate that all of the elements (barring
204 Cu and Pb in the Yicheng area) are characterized by a wide range of α values with
205 $\tau''(1)$ values less than -0.01 and $\Delta f(\alpha)$ values larger than 0.5 , all of which indicate that
206 these elements have a high multifractality within the soils in these two areas. All of
207 the elements analyzed during this study (barring Hg) have higher $\Delta f(\alpha)$ and α values
208 (except Zn) and lower $\tau''(1)$ values in soils from the Daxing area, with Hg having
209 higher $\Delta f(\alpha)$ and $\Delta\alpha$ and lower $\tau''(1)$ values in soils from the Yicheng area (Table 2).
210 This suggests that the industrial activities in the Daxing area generate multi-element
211 heavy metal soil contamination, whereas the most significant heavy metal pollution
212 associated with the agricultural activity in the Yicheng area is Hg contamination. The
213 $\Delta f(\alpha)$ and $\Delta\alpha$ values of Hg in the Yicheng area are larger than the values for all other
214 elements in this area as well as some of the elements in the Daxing area, indicating
215 both the prevalence and significant degree of agricultural Hg contamination in the
216 Yicheng area, even considering the lower overall concentrations of Hg within the
217 Yicheng area compared to the Daxing area. This contamination should be considered
218 a priority in terms of remediation, because the interaction between the agricultural
219 activity in the Yicheng area and this Hg pollution could seriously impact human
220 health, as Hg is preferentially concentrated upward in the food chain (e.g. (Jiang et al.,
221 2006)). This means that although contamination in both areas needs to be evaluated
222 further and should be remediated to avoid any deleterious effects, the fact that the Hg
223 contamination in the Yicheng area may be more bioavailable and may have a larger
224 effect on the population of this region (as a result of the agricultural activity in this
225 area) means it should be considered a priority.

226

227

228

229 **Table 2.** Multifractal parameters of the elements analyzed during this study.

Town	Element	α_{\min}	α_{\max}	$\Delta\alpha_L$	$\Delta\alpha_R$	$\Delta\alpha$	$\Delta f(\alpha)$	$\tau''(1)$
Daxing	Cu	1.733	2.057	0.280	0.044	0.324	1.270	-0.015
	Pb	1.439	2.050	0.567	0.044	0.611	1.659	-0.068
	Zn	1.733	2.109	0.288	0.088	0.376	0.841	-0.066
	Cd	1.482	2.285	0.499	0.304	0.803	1.358	-0.066
	As	1.285	2.094	0.739	0.070	0.809	1.490	-0.243
	Hg	1.780	2.191	0.248	0.163	0.411	0.656	-0.079
Yicheng	Cu	1.971	2.067	0.036	0.060	0.096	0.168	-0.007
	Pb	1.900	2.062	0.104	0.058	0.162	0.646	-0.005
	Zn	1.729	2.112	0.275	0.108	0.383	1.275	-0.016
	Cd	1.800	2.103	0.201	0.102	0.303	0.829	-0.023
	As	1.659	2.076	0.343	0.075	0.418	1.224	-0.036
	Hg	1.507	2.084	0.497	0.080	0.577	1.243	-0.096

230

231 In order to compare variations in multifractality, the elements within the samples
 232 from Daxing and Yicheng area were sorted by $\Delta\alpha$, $\Delta f(\alpha)$ and $\tau''(1)$ parameters,
 233 respectively, in addition to sorting by coefficient of variation values (Table 3). The
 234 data shown in Table 3 indicates that the Pb data within the Daxing area has close to
 235 the lowest coefficient of variation, but largest the $\Delta f(\alpha)$ and $\tau''(1)$ values for these Pb
 236 data are indicative of strongest multifractality compared to the other heavy metals in
 237 the soils within the Daxing area. In comparison, the As data for soils in the Daxing
 238 area yielded the largest coefficient of variation but the moderate $\Delta f(\alpha)$ and $\tau''(1)$
 239 values, indicating these As data only have moderate multifractality. These differences
 240 indicate that the multifractal parameters reveal new information about the nonlinear
 241 variability and the characteristics of these geochemical data compared to the basic
 242 statistics for these samples. In addition, the data given in Table 3 indicates that these
 243 elements have different orders depending on whether they are sorted by $\Delta\alpha$, $\Delta f(\alpha)$ or
 244 by $\tau''(1)$ values, all of which reflects differing aspects of the multifractality of these
 245 data. Here we consider that $\Delta\alpha$, $\Delta f(\alpha)$ or by $\tau''(1)$ have equal weightings that reflect
 246 the overall multifractality of the data from the study area. As such, the ordering of
 247 these elements by $\Delta\alpha$, $\Delta f(\alpha)$ or by $\tau''(1)$ involved the summation of these values with
 248 the summed ordering then sorted again to compare the overall multifractality of these
 249 data.

250 **Table 3.** Elements sorted by multifractal parameters and basic statistic indices.

Town	Element	Order				
		Basic statistics	Multifractal parameters			
		Coefficient of variation	$\Delta\alpha$	$\Delta f(\alpha)$	$\tau''(1)$	Overall*
Daxing	Cu	6	6	4	6	6
	Pb	5	3	1	1	1
	Zn	4	5	5	2	4
	Cd	2	2	3	3	2
	As	1	1	2	5	3
	Hg	3	4	6	4	5
Yicheng	Cu	5	6	6	5	6
	Pb	6	5	5	6	5
	Zn	4	3	1	4	3
	Cd	3	4	4	3	4
	As	2	2	3	2	2
	Hg	1	1	2	1	1

251 Overall: the overall order of $\Delta\alpha$, $\Delta f(\alpha)$ and $\tau''(1)$.

252

253 The overall amount of multifractality within the soil geochemical data for the
 254 Daxing area decreases as follows: Pb>Cd>As>Zn>Hg>Cu, whereas the overall
 255 amount of multifractality within the soil geochemical data for the Yicheng area
 256 decreases as follows: Hg>As>Zn>Cd>Pb>Cu. The overall orders indicate that the Pb
 257 and Hg soil data have the highest degree of multifractality in the Daxing and Yicheng
 258 areas, respectively, whereas Cu has the weakest multifractality irrespective of the
 259 area.

260 We further analyzed the spatial distribution of contamination within soils from
 261 the Daxing and Yicheng areas and evaluated whether there is any significant
 262 correlation between multifractality and anthropogenic activity. Filled contour maps
 263 showing the distribution of Pb in the Daxing area and Hg and Cu in the Yicheng area
 264 were calculated using inverse distance weighted interpolation (Fig. 4–6). These
 265 figures show that areas with elevated levels of Pb contamination within the Daxing
 266 area are correlated with the location of industrial factories, although interestingly the
 267 areas in the upper and lower left hand side of Fig. 4 contain factories but not elevated
 268 concentrations of Pb. This indicates that the Pb concentrations in these soils may be
 269 dependent on both the presence and type of industry in this area, with some industries

270 polluting more than others, either as a direct result of the differing industries present
271 in this area or as a result of differing (or a lack of in some areas) approaches to
272 lessening environmental impacts. In comparison, the Hg contamination in the Yicheng
273 area is definitely spatially correlated with the location of agricultural breeding
274 facilities. Although the mean concentrations of Hg in soils are greater in the Daxing
275 area, all of the multifractal parameters determined during this study ($\Delta\alpha$, $\Delta f(\alpha)$ and
276 $\tau''(1)$) indicate that the Hg data in the Daxing area has a lower multifractality than
277 the Hg data in the Yicheng area. The Yicheng area is heavily agricultural, meaning
278 that the agricultural activities in this area may be both concentrating Hg as well as
279 contaminating soils. In addition, although the mean concentrations of Hg in the
280 Yicheng area are lower than in the soils in the Daxing area, the former has a higher
281 maximum concentration than the latter, and both areas have significant Hg
282 contamination. Indeed, the contamination in the Yicheng area may be of more concern
283 than the contamination in the Daxing area, as the agricultural activity in the Yicheng
284 area may lead to greater human intake of Hg than from the soils in the mainly
285 industrial Daxing area, a factor that could lead to serious health issues (e.g. Minamata
286 disease) caused by the potential concentration of Hg up the food chain. This indicates
287 that soils in both areas may well require control and remediation.

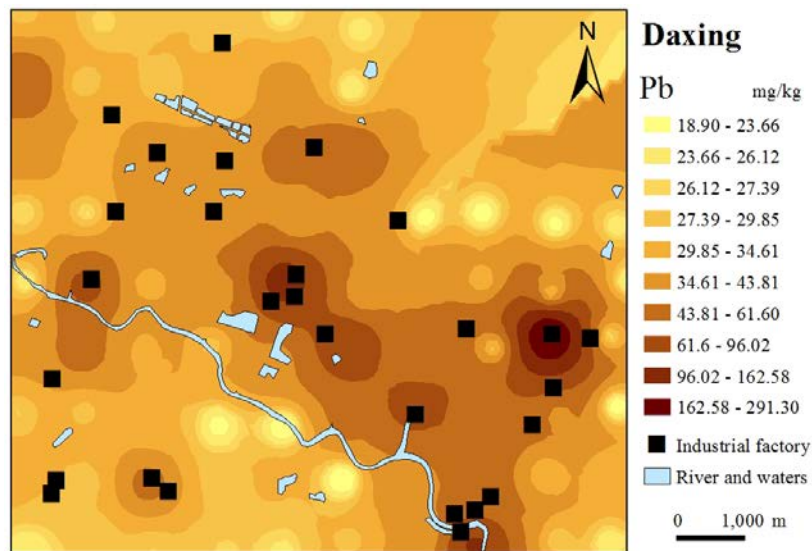
288 This distribution of soils with elevated concentrations of Hg also contrasts with
289 the symmetrical distribution and weakest multifractality for Cu within the Yicheng
290 area (Fig. 3, 5-6). Here, we generated a correlation matrix that compares the
291 relationship between the spatial density of breeding locations in the Yicheng area (Fig.
292 7) and filled contours maps showing the distribution of Hg (Fig. 5) and Cu (Fig. 6) in
293 this region to identify whether there are any spatial correlations between the location
294 of agricultural facilities and areas containing soils with elevated heavy metal
295 concentrations (Table 4). The correlation matrix shows a significant correlation
296 between agricultural facilities and high concentrations of Hg (coefficient of
297 correlation = 0.434), whereas the location of these agricultural breeding facilities and
298 areas of high Cu concentrations either have no relationship or are negatively
299 correlated (coefficient of correlation = -0.064). This indicates that very little Cu has

300 been anthropogenically added (or removed) from the soils in the Yicheng area,
301 suggesting that these soils may contain only natural background concentrations of Cu
302 and that the breeding facilities in this area do not produce significant Cu
303 contamination. The negative correlation coefficient, symmetrical distribution and
304 weakest multifractality of Cu give one clue to the spatial relationship between Cu
305 contamination and the river in the right hand side of Fig. 6. This may suggest a
306 non-anthropogenic source (e.g. flooding causing the deposition of Cu or some other
307 relationship between water and Cu contamination) for some of the slightly elevated
308 Cu concentrations in this region. In addition, the fact that some breeding facilities are
309 not associated with significant Hg contamination (Fig. 5) suggests again that although
310 there is a relationship between the presence of these facilities and contamination, it
311 may be that the Hg contamination in this area reflects differing types of breeding
312 facilities or differing (or a lack of) approaches to lessening environmental impacts.

313 These results indicate that multifractal modeling and the associated generation of
314 multifractal parameters are a useful approach in the evaluation of heavy metal
315 pollution in soils and the identification of major element of heavy metal
316 contamination. In addition, the differing orders of the multifractality of the
317 geochemical data for soils within the Daxing area and Yicheng area are indicative of a
318 significant difference in the geochemical characteristics (and heavy metal pollution)
319 in the soils within these two areas. This indicates that differing treatment strategy and
320 clean-up approaches to remediating these two polluted areas are needed, rather than a
321 single cover-all strategy and approach to the remediation of heavy metal pollution. A
322 significant number of different remediation approaches can be used to resolve the
323 issues of heavy metal soil contamination (e.g., Bech et al., 2014; Koptsik, 2014).
324 Although somewhat beyond the scope of this study, the multi-element nature of the
325 contamination in the Daxing area means that physical and chemical approaches to
326 remediation (i.e., soil removal, soil vitrification, soil consolidation, electroremediation,
327 or soil washing) are probably well suited for the remediation of heavy metal
328 contaminated soil in this region (especially Pb). In comparison, the differing (i.e.
329 Hg-dominated) type of soil contamination in the Yicheng area could be more

330 efficiently treated using microremediation and phytoremediation, primarily as the
331 agriculture in this area requires a rapid reduction in the mobility and biological
332 availability of heavy metals in the soils (Mulligan et al., 2001; Wang and Greger,
333 2006). In addition, the source of the Hg contamination (e.g. fertilizer, fodder,
334 pesticides, water) remains unclear. Identifying this source is also beyond the scope of
335 this paper although it is also clearly an area for future research, as the identification of
336 the source or sources of this contamination may prevent the future heavy metal
337 pollution of soils in this region.

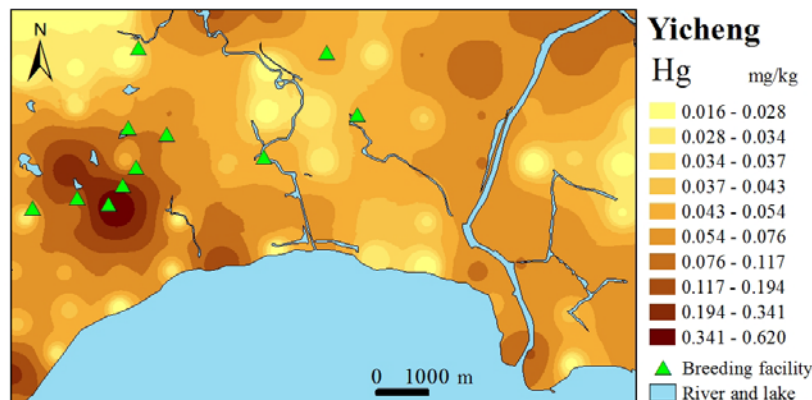
338



339

340 **Fig. 4.** Filled contour map generated by inverse distance weighted interpolation showing the
341 spatial distribution of soil Pb concentrations in the Daxing area (generated using Inverse Distance
342 Weighted Interpolation method within spatial analyst tools of the ArcGIS software package).

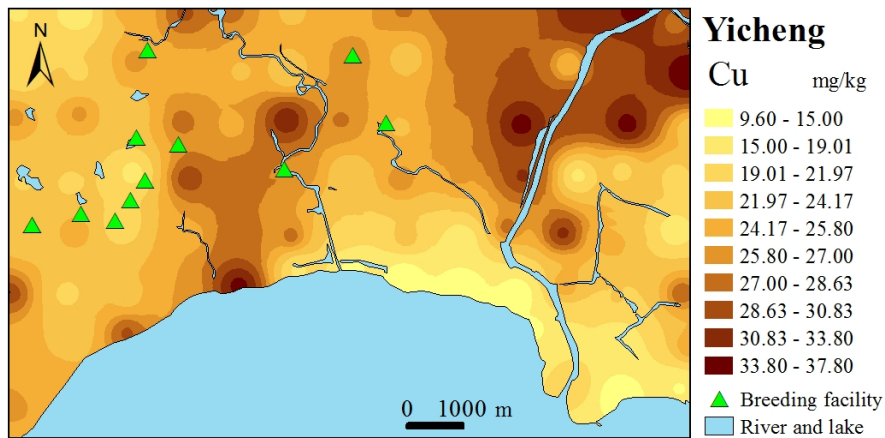
343



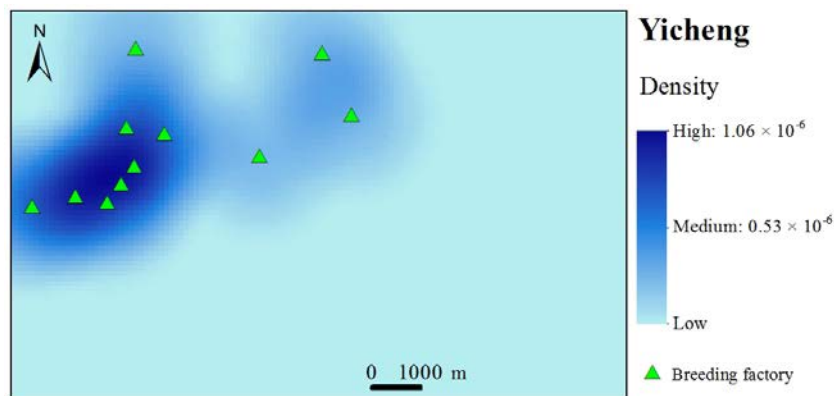
344

345 **Fig. 5.** Filled contour map generated by inverse distance weighted interpolation showing the
346 spatial distribution of soil Hg concentrations in the Yicheng area (generated using Inverse

347 Distance Weighted Interpolation method within spatial analyst tools of the ArcGIS software
 348 package).
 349



350
 351 **Fig. 6.** Filled contour map generated by inverse distance weighted interpolation showing the
 352 spatial distribution of soil Cu concentrations and the location of breeding facilities in the Yicheng
 353 area (generated using Inverse Distance Weighted Interpolation method within spatial analyst tools
 354 of the ArcGIS software package).
 355



356
 357 **Fig. 7.** Density map of breeding facilities in Yicheng area (generated using the Kernel
 358 Density method within spatial analyst tools of the ArcGIS software package).
 359

360 **Table 4.** Correlation matrix comparing the breeding facility density map and the filled contour
 361 maps for Hg and Cu data for the Yicheng area (calculated using the Band Collection Statistics
 362 within spatial analyst tools of the ArcGIS software package).

Layers	Layer 1	Layer 2	Layer 3
Layer 1	1.000	0.434	-0.064
Layer 2	0.434	1.000	-0.464
Layer 3	-0.064	-0.464	1.000

363 Layer 1: Density map of breeding factories of Yicheng area (Fig. 7);
 364 Layer 2: Filled contour map of Hg concentrations of Yicheng area (Fig. 5);
 365 Layer 3: Filled contour map of Cu concentrations of Yicheng area (Fig. 6).
 366

367 **5. Conclusions**

368 Multifractal modelling and the resulting multifractal parameters in this paper
369 indicate that the soils from the Daxing area have stronger multifractality for Cu, Pb,
370 Zn, Cd and As than soils from the Yicheng area, although the latter have relatively
371 strong multifractality for Hg. The ordering of values for the multifractal parameters
372 $\Delta\alpha$, $\Delta f(\alpha)$ and $\tau''(1)$ indicate the degree of multifractality for the geochemical data for
373 soils within the Daxing area descends as follows: Pb>Cd>As>Zn>Hg>Cu, whereas
374 within the Yicheng area descends as follows: Hg>As>Zn>Cd>Pb>Cu. In addition, Cu
375 concentrations in soils in the Yicheng area may still have their original (i.e. natural)
376 distribution and may not have been influenced by human activities. These data
377 indicate that the industrial activity concentrated in the Daxing area generates
378 multi-element heavy metal soil contamination whereas the agricultural activity
379 concentrated in the Yicheng area generates Hg-dominated heavy metal soil
380 contamination. The latter is important, as Hg contamination can cause serious health
381 issues (e.g. Minamata disease) and the soils in this area may require remediation,
382 especially as Hg can be concentrated up the food chain and the Yicheng area is
383 heavily agricultural, indicating that this activity may both be concentrating Hg as well
384 as contaminating soils in this area.

385 The results presented here indicate that multifractal modeling can be a useful
386 approach in the evaluation of heavy metal pollution in soils and the identification of
387 problematic heavy metals that need remediation in the research area.

388

389 **Acknowledgements**

390 This research was financially supported by funds from the China Academy of
391 Science "Light of West China" Program, the Fundamental Research Funds for the
392 Central Universities, and the Programme for New Century Excellent Talents in
393 University (Grant No. NCET-10-0324).

394

395

396 **References**

- 397 Albanese, S., De Vivo, B., Lima, A., and Cicchella, D.: Geochemical background and
398 baseline values of toxic elements in stream sediments of Campania region (Italy),
399 J. Geochem. Explor., 93, 21-34, 2007.
- 400 Armstrong, H. E. L., Corns, W. T., Stockwell, P. B., O'Connor, G., Ebdon, L., and
401 Evans, E. H.: Comparison of afs and icp-ms detection coupled with gas
402 chromatography for the determination of methylmercury in marine samples. Anal.
403 Chim. Acta., 390, 245-253,1999.
- 404 Bech, J., Korobova, E., Abreu, M., Bini, C., Chon, H. T., and Pérez-Sirvent, C.: Soil
405 pollution and reclamation, J. Geochem. Explor., 147, 77-79, 2014.
- 406 Buczkowski, S., Hildgen, P., and Cartilier, L.: Measurements of fractal dimension by
407 box-counting: a critical analysis of data scatter, Physica A Statistical Mechanics &
408 Its Applications, 252, 23–34, 1998.
- 409 Caniego, F. J., Espejo, R., Martín, M. A., and José, F. S.: Multifractal scaling of soil
410 spatial variability, Ecol. Model., 182, 291-303, 2005.
- 411 Cheng, Q.: The perimeter-area fractal model and its application to geology, Math.
412 Geol., 27, 69-82, 1995.
- 413 Cheng, Q.: The gliding box method for multifractal modeling, Comput. Geosci., 25,
414 1073-1079, 1999.
- 415 Cheng, Q.: Selection of Multifractal Scaling Breaks and Separation of Geochemical
416 and Geophysical Anomaly, Journal of China University of Geosciences, 1, 54-59,
417 2001.
- 418 Cheng, Q.: Multifractal modelling and spectrum analysis: Methods and applications to
419 gamma ray spectrometer data from southwestern Nova Scotia, Canada, Sci. China.
420 Ser. D, 49, 283-294, 2006.
- 421 Dathe, A., Tarquis, A. M., and Perrier, E.: Multifractal analysis of the pore- and
422 solid-phases in binary two-dimensional images of natural porous structures,
423 Geoderma, 134, 318–326, 2006.
- 424 Deng, J., Wang, Q., Wan, L., Liu, H., Yang, L., and Zhang, J.: A multifractal analysis

425 of mineralization characteristics of the Dayingezhuang disseminated-veinlet gold
426 deposit in the Jiaodong gold province of China, *Ore Geol. Rev.*, 40, 54–64, 2011.

427 Gómez-Ariza, J. L., Sánchez-Rodas, D., Giráldez, I., and Morales, E.: A comparison
428 between ICP-MS and AFS detection for arsenic speciation in environmental
429 samples, *Talanta*, 51, 257-268, 2000.

430 Gonçalves, M. A.: Characterization of Geochemical Distributions Using Multifractal
431 Models, *Math. Geol.*, 33, 41-61, 2000.

432 Guillén, M. T., Delgado, J., Albanese, S., Nieto, J. M., Lima, A., and De Vivo, B.:
433 Environmental geochemical mapping of Huelva municipality soils (SW Spain) as
434 a tool to determine background and baseline values, *J. Geochem. Explor.*, 109,
435 59-69, 2011.

436 Jennane, R., Ohley, W. J., Majumdar, S., and Lemineur, G.: Fractal analysis of bone
437 X-ray tomographic microscopy projections, *IEEE T. Med. Imaging*, 20, 443-449,
438 2001.

439 Jiang, G. B., Shi, J. B., and Feng, X. B.: Mercury Pollution in China, *Environ. Sci.*
440 *Technol.*, 40, 3672-3678, 2006.

441 Koptsik, G. N.: Modern approaches to remediation of heavy metal polluted soils: A
442 review, *Eurasian Soil. Sci.*, 47, 707-722, 2014. †

443 Kravchenko, A., Boast, C., and Bullock, D.: Multifractal analysis of soil spatial
444 variability, *Agron. J.*, 91, 1033-1041, 1999.

445 Leyval, C., Turnau, K., and Haselwandter, K.: Effect of heavy metal pollution on
446 mycorrhizal colonization and function: physiological, ecological and applied
447 aspects, *Mycorrhiza*, 7, 139-153, 1997.

448 Lima, A., De Vivo, B., Cicchella, D., Cortini, M., and Albanese, S.: Multifractal IDW
449 interpolation and fractal filtering method in environmental studies: an application
450 on regional stream sediments of (Italy), Campania region, *Appl. Geochem.*, 18,
451 1853-1865, 2003.

452 Lopes, R., and Betrouni, N.: Fractal and multifractal analysis: A review, *Med. Image.*
453 *Anal.*, 13, 634-649, 2009.

454 Luo, C., Liu, C., Yan, W., Xiang, L., Li, F., Gan, Z., and Li, X.: Heavy metal

455 contamination in soils and vegetables near an e-waste processing site, South
456 China, *J. Hazard. Mater.*, 186, 481-490, 2011.

457 McGrath, D., Zhang, C., and Carton, O. T.: Geostatistical analyses and hazard
458 assessment on soil lead in Silvermines area, Ireland, *Environ. Pollut.*, 127,
459 239-248, 2004.

460 Mulligan, C., Yong, R., and Gibbs, B. F.: Remediation technologies for
461 metal-contaminated soils and groundwater: an evaluation. *Eng. Geol.*, 60,
462 193-207, 2001.

463 Pascual, M., Ascioti, F., and Caswell, H.: Intermittency in the plankton: a multifractal
464 analysis of zooplankton biomass variability, *J. Plankton Res.*, 17, 167-168, 1995.

465 Salvadori, G., Ratti, S. P., and Belli, G.: Fractal and multifractal approach to
466 environmental pollution, *Environ. Sci. Pollut. R.*, 4, 91-98, 1997.

467 Schertzer, D., Lovejoy, S., Schmitt, F., Chigirinskaya, Y., and Marsan, D.: Multifractal
468 Cascade Dynamics and Turbulent Intermittency, *Fractal. s.*, 5, 427-471, 2011.

469 Tarquis, A. M., McInnes, K. J., Key, J. R., Saa, A., García, M. R., and Díaz, M. C.:
470 Multiscaling analysis in a structured clay soil using 2D images, *J. Hydrol.*, 322,
471 236-246, 2006.

472 Thomas, K., and Stefan, S.: Estimate of heavy metal contamination in soils after a
473 mining accident using reflectance spectroscopy, *Environ. Sci. Technol.*, 36,
474 2742-2747, 2002.

475 Wang, Y., and Greger, M.: Use of iodide to enhance the phytoextraction of
476 mercury-contaminated soil. *Sci. Total. Environ.*, 368, 30-39, 2006.

477 Wang, Y. P., Shi, J. Y., Wang, H., Lin, Q., Chen, X. C., and Chen, Y. X.: The influence
478 of soil heavy metals pollution on soil microbial biomass, enzyme activity, and
479 community composition near a copper smelter. *Ecotox Environ Safe, Ecotox.*
480 *Environ. Safe.*, 67, 75-81, 2007.

481 Wendt, H., Roux, S. G., Jaffard, S., and Abry, P.: Wavelet leaders and bootstrap for
482 multifractal analysis of images, *Signal Process.*, 89, 1100–1114, 2009.

483 Xie, S., Cheng, Q., Xing, X., Bao, Z., and Chen, Z.: Geochemical multifractal
484 distribution patterns in sediments from ordered streams, *Geoderma*, 160, 36-46,

485 2010.

486 Yuan, F., Li, X., Jowitt, S. M., Zhang, M., Jia, C., Bai, X., and Zhou, T.: Anomaly
487 identification in soil geochemistry using multifractal interpolation: A case study
488 using the distribution of Cu and Au in soils from the Tongling mining district,
489 Yangtze metallogenic belt, Anhui province, China, *J. Geochem. Explor.*, 116-117,
490 28-39, 2012.

491 Yuan, F., Li, X., Zhou, T., Deng, Y., Zhang, D., Xu, C., Zhang, R., Jia, C., and Jowitt,
492 S. M.: Multifractal modelling-based mapping and identification of geochemical
493 anomalies associated with Cu and Au mineralisation in the NW Junggar area of
494 northern Xinjiang Province, China, *J. Geochem. Explor.*, 154, 252-264, 2015.

495 Zuo, R., Carranza, E. J. M., and Cheng, Q.: Fractal/multifractal modelling of
496 geochemical exploration data, *J. Geochem. Explor.*, 122, 1-3, 2012.

497